Polish Society of Composite Materials
Polskie Towarzystwo Materiałów Kompozytowych

15: 3 (2015) 174-180

COMPOSITES THEORY AND PRACTICE

Justyna Stolarska, Jan Dutkiewicz, Wojciech Maziarz*, Janusz Pstruś, Anna Wójcik, Piotr Ozga

Institute of Metallurgy and Materials Science PAS, ul. Reymonta 25, 30-059 Kraków, Poland
**Corresponding author: E-mail: w.maziarz@imim.pl*

Received (Otrzymano) 20.04.2015

COPPER MATRIX COMPOSITES STRENGTHENED WITH CARBON NANOTUBES OR GRAPHENE PLATELETS PREPARED BY BALL MILLING AND VACUUM HOT PRESSING

In this study copper matrix composites with two types of additions i.e. graphene platelets in the amount of 1÷2 wt.% or multiwall carbon nanotubes in the amount of 1÷3 wt.% were studied. Two types of graphene platelets were applied: of a fine thickness of 2÷4 nm and coarser of a 10÷20 nm plate thickness. The addition of finer graphene platelets to copper causes less strengthening, but smaller electrical resistivity, while the addition of MWCNTs causes an increase in hardness in comparison to graphene platelets and slightly higher resistivity growing with the amount of nanotubes. SEM and TEM studies allowed to determine that carbon nanotubes and copper grain size are refined during milling which does not change after consolidation. In the samples with graphene, a more homogeneous distribution of platelets was observed in the case of fine graphene, while platelet conglomerates in the case of coarser graphene tend to occur after the consolidation process at the copper particle boundaries.

Keywords: copper composites, carbon nanotubes, graphene platelets, electron microscopy

KOMPOZYTY NA OSNOWIE MIEDZI WZMACNIANE NANORURKAMI WĘGLOWYMI LUB PŁATKAMI GRAFENOWYMI WYTWORZONE POPRZEZ MIELENIE PROSZKÓW I PRASOWANIE NA GORĄCO W PRÓŻNI

W niniejszej pracy opracowano sposób wytworzenia kompozytów na osnowie miedzi, wzmacnianych różnymi typami węgla, tj. wielościennymi nanorurkami węglowymi w ilości 1÷3% obj. oraz płatkami grafenowymi w ilości 1÷2% wag. Wytypowano dwa rodzaje płytek grafenowych dostępnych komercyjnie pod nazwą: N006 o grubości 10÷20 mm oraz cieńsze FL-RGO o grubości 2÷4 mm. Dodawanie drobniejszych płatków grafenowych do miedzi powoduje mniejsze umocnienie i mniejszy opór elektryczny, natomiast dodanie wielościennych nanorurek węglowych (MWCNTs) powoduje wzrost twardości w porównaniu do płatków grafenu i niewiele większą oporność wzrastającą wraz z ilością nanorurek. Badania na skaningowym mikroskopie elektronowym SEM oraz transmisyjnym mikroskopie elektronowym TEM pozwoliły ustalić, że mieszanina MWCNTs oraz proszku miedzi podczas mielenia w młynie kulowym zmienia się, tworząc najpierw duże konglomeraty, a po 32 godzinach mniejsze ziarna miedzi oraz rozdrobnione nanorurki. Ponadto analiza badań ze spektroskopii Ramanowskiej ujawniła, że nanorurki węglowe ulegają pewnego rodzaju deformacji, zwiększając tym samym stopień zdefektowania. W kompozytach z dodatkiem grafenu stwierdzono bardziej jednorodny rozkład płatków w ziarnach miedzi w przypadku drobnego grafenu, podczas gdy w przypadku grubszych płatków grafenu tworzą się konglomeraty, które po procesie konsolidacji występują na granicach cząstek proszku miedzi.

Słowa kluczowe: kompozyty metalowe, mikrostruktura, struktura gradientowa, kompozyty odlewane

INTRODUCTION

The new structural forms of carbon like graphene or nanotubes show a high mechanical strength as well as high electrical and thermal conductivity. They are therefore of interest as composite components, particularly polymer or metal based ones [1-15]. Metal-based composites with carbonaceous nanomaterials can achieve optimal mechanical and physical properties if the reinforcements are dispersed uniformly in the matrix. Ball milling appears to be an effective process for achieving better dispersion of nanofillers in the metal matrix [1-15]. In Cu-based nanocomposites, low volume fractions (1-4 wt.%) of nanofillers are used to achieve the required high thermal conductivity and mechanical strength [1-4, 7]. The wear rate and hardness of composites strengthened with CNTs (carbon nanotubes) increases up to 15% of their volume fraction and then decreases [5]. The majority of CNT/Cu composites are mainly fabricated by means of the PM

(powder metallurgy) processing route [1-7, 9, 13-15]. Interfacial amorphous layers, probably originating from Cu oxide in the Cu powders and amorphous carbon on the surface of the CNTs, were observed in the CNT-Cu composite matrix. They act as a thermal barrier and due to the relatively large thermal resistance of these layers, MWCNTs are expected to act like elongated pores [6]. The preparation of a copper-carbon composite is possible by: thermal spraying, powder metallurgy, hot extrusion or electrodeposition [1-15]. The additions of CNT or graphene enhance the stiffness and strength of the resulting composites markedly. Furthermore, the incorporation of flexible CNTs with a very high strain-to-failure in metals/alloys only leads to a small reduction or even an increase in their tensile ductility. Due to the high thermal conductivity of CNT or graphene, the potential of these nanomaterials serving as thermal conductors has not yet been fully realized. In order to fabricate composites containing carbon nanotubes, powder metallurgy is often used, where the matrix is aluminum, copper or other metals like Mg, Ti and Ni. This technique is important because one can easily achieve good dispersion of CNT in the matrix. It is expected that a small size of powders with an appropriate dispersion of CNT can prevent oxidation. Mechanical alloying also leads to deformation and welding CNTs with other mixing powders. High density of the composite can be received by hot pressing. In this process, carbon nanotubes are flattened by temperature and pressure. The necessary time to achieve good density of the composite is 1h during hot pressing [1]. Composites strengthened with carbon nanotubes have applications in space telescopes, due to their light weight and long lifetime [1].

The aim of the present paper was to compare the basic mechanical properties and electrical conductivity of copper matrix composites strengthened with either carbon nanotubes or graphene platelets of various thickness and to correlate their microstructures with the obtained properties.

EXPERIMENTAL PROCEDURE

As the starting material for the preparation of copper matrix composites, pure copper powders (purity no less than 99.9%) were used, with additions of multi wall carbon nanotubes (MWCNT) or graphene platelets of two different types. Commercially available N006 graphene platelets with a plate thickness of 10÷20 nm produced by Angstron Materials USA and much finer graphene platelets FLRGO with a plate thickness of 2÷4 nm produced by Nanomaterials SA Warsaw were added. Mixtures of the copper powders and the strengthening particles with compositions as presented in Table 1 were prepared under argon atmosphere in a glove box. Then they were milled for 5 hours using a planetary ball mill Fritsch Pulverisette 5 at the rotation rate 200 rpm.

TABLE 1. **Characteristics of graphene platelets, carbon nanotubes and composite compositions**

TABELA 1. **Charakterystyki płatków grafenu i nanorurek węglowych oraz skład chemiczny badanych kompozytów**

	Graphene N006	**Graphene FL-RGOMWCNTMWCNT**		
dimensions	thickness 10÷20 nm	thickness <4 nm max. 10 mono-layers	outside diameter: 30-50 nm, inside diameter: 5-15 nm, length: 10-20 um	outside diameter: 30÷50 nm, inside diameter: 5÷15 nm, length: 10÷20 um
Mixing time	5 hours	5 hours	8 hours 32 hours	5 hours
Addition to copper	1% (0.55 g) and 2% (1.1 g) weight	1% (0.55 g) and 2% (1.1 g) weight	1% (0.14 g) and 3% (0.42 g) volume	1% (0.55 g) weight

Zirconia containers and balls were used in order to prevent contamination and the ratio of ball mass to powder mass was 10:1. Composite samples of 20 mm in diameter and 5 mm high were produced using uniaxial hot pressing in vacuum of 10^{-2} bar. The sintering temperature was chosen as 510°C, pressure 550 MPa and the time of keeping samples in these conditions was 30 min. The structure and composition were studied using a Philips CM20 or FEI Technai G2 transmission electron microscope (TEM) and a Quanta 3D FEG scanning electron microscope (SEM). Thin samples of graphene powders were observed on holey carbon foil, while those of the bulk samples were cut by a diamond saw, followed by dimpling using a Gatan dimpler and ion beam thinning in a Leica EM RES101 ion beam thinner. X-ray diffraction was performed using a Philips PW1710 diffractometer with CoKα radiation. The hardness was measured using a Zwick ZHU250 instrument. The electrical resistivity was measured using the 4-point contact method. Micro-Raman spectra were taken using a Renishaw in a Via Raman microscope (100x objective) with a 633 nm HeNe excitation laser, 1s exposure time, 50 accumulations, and 100% laser power (21 mW output power), with spatial resolution <1 μm.

RESULTS AND DISCUSSION

Characterization of starting material

Microscopy techniques were used to characterize the starting material. Figure 1 presents the bright field (BF) TEM and secondary electron (SE) SEM microstructure of the MWCNT and copper powders, respectively, both in as-delivered condition. One can see in the BF image that MWCNTs have an irregular outer surface and their length is 10÷20 μm. The copper powder particles range in size from 10 to 50 μm and mainly

have a spherical shape. The high resolution (HREM) TEM microstructure of MWCNT and its Raman spectra are presented in Figure 2. The HREM image and corresponding fast Fourier transform (FFT) show that the walls consist of several parallel planes with interplanar spacing equal to d = 0.351 nm which is very close to (002) graphite planes (d = 0.335 nm). The inverse fast Fourier transform (IFFT) image obtained after the masking procedure presents $(002)_g$ parallel planes with a high density of structural faults. By applying the line profile of intensities in the perpendicular direction to the planes, it is possible to estimate the outer and inner diameter of the tubes. It was measured that the outside diameter of the tubes is between 30 and 50 nm whereas the inner between is 5 to 15 nm, which is in good agreement with that declared by the producer.

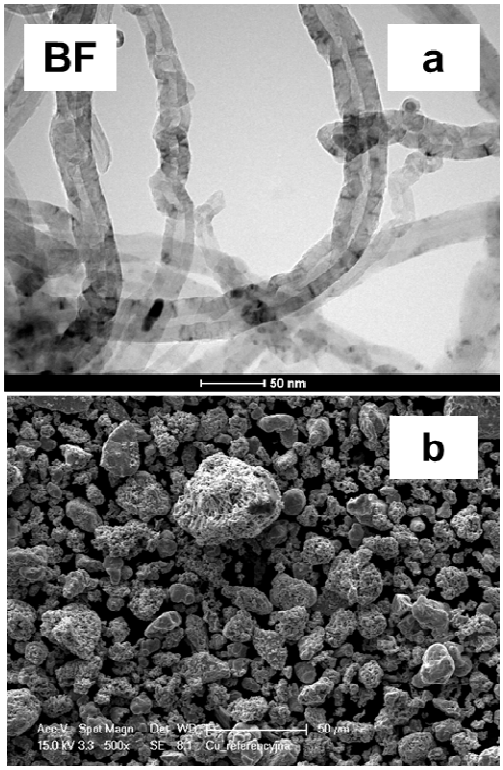

Fig. 1. BF TEM (a) and SE SEM (b) microstructure of MWCNT and copper powders, respectively, both in as-delivered condition

Rys. 1. BF TEM (a) i SE SEM (b) mikrostruktury nanorurek węglowych i proszku miedzi w stanie dostarczonym

The high level of structural defects in the as-delivered MWCNTs was also confirmed by Raman spectroscopy investigations. The ratio of intensities of D bands (I(D)) and G bands (I(G)) equal to 2.07 indicates that MWCNT are highly defected. Simultaneous broadening of the G peak (47 cm^{-1}) also suggests a significant amount of an amorphous carbon.

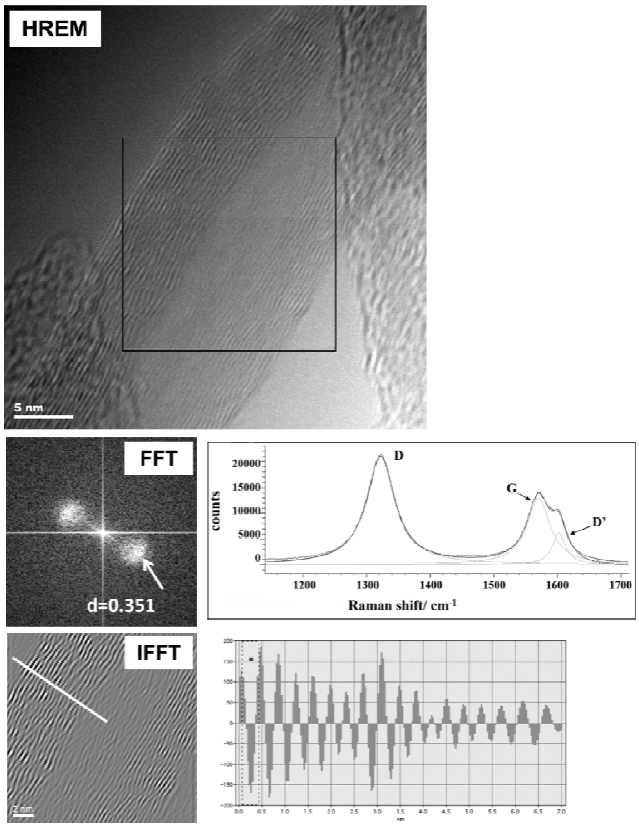

Fig. 2. HREM TEM microstructure and Raman spectra of MWCNT in as-delivered condition

Rys. 2. Mikrostruktura wysokorozdzielcza HREM TEM i spektrum Ramanowskie nanorurek węglowych w stanie dostarczonym

Figure 3 shows TEM micrographs taken of N006 graphene platelets showing agglomerates in (a) and the thickness of a platelet at a higher magnification in (b) showing platelet thickness between 10÷20 nm according to the specification of Angstron materials. The selected area diffraction pattern (SADP) in Figure 3c shows interplanar distances characteristic for graphite.

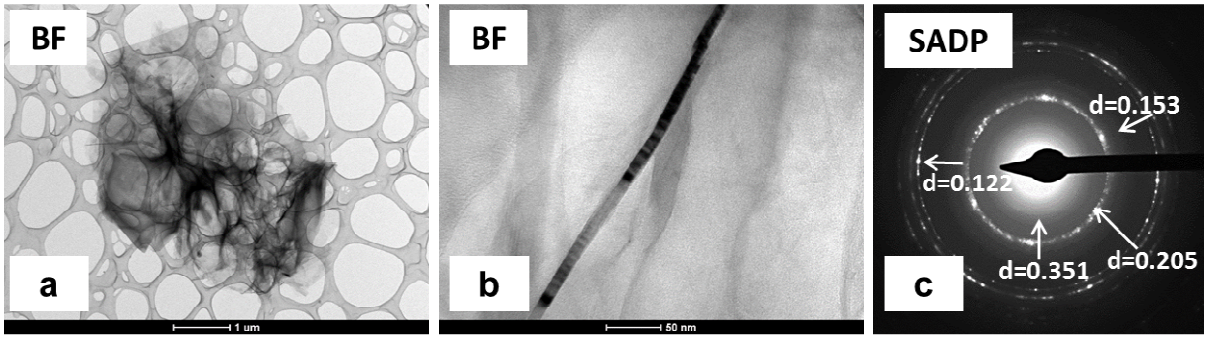

Fig. 3. BF TEM (a and b) micrographs from N006 graphene platelets and SADP (c) showing graphite interplanar distances

Rys. 3. Mikrostruktury TEM (a i b) w jasnym polu (BF) płatków grafenu N006 oraz dyfrakcja elektronowa (SADP) (c) pokazująca odległości międzypłaszczyznowe grafitu

Figure 4 shows TEM micrographs of the FLRGO graphene platelets. They are composed of several layers of platelets show in the plane perpendicular to the platelet. Its thickness scan be not clearly seen, however, it is close to the specification between 2÷4 nm, which was confirmed by the Raman studies. The diffraction pattern is different than that in Figure 3 showing only diffused reflection 002 due to the fine shape of the platelets.

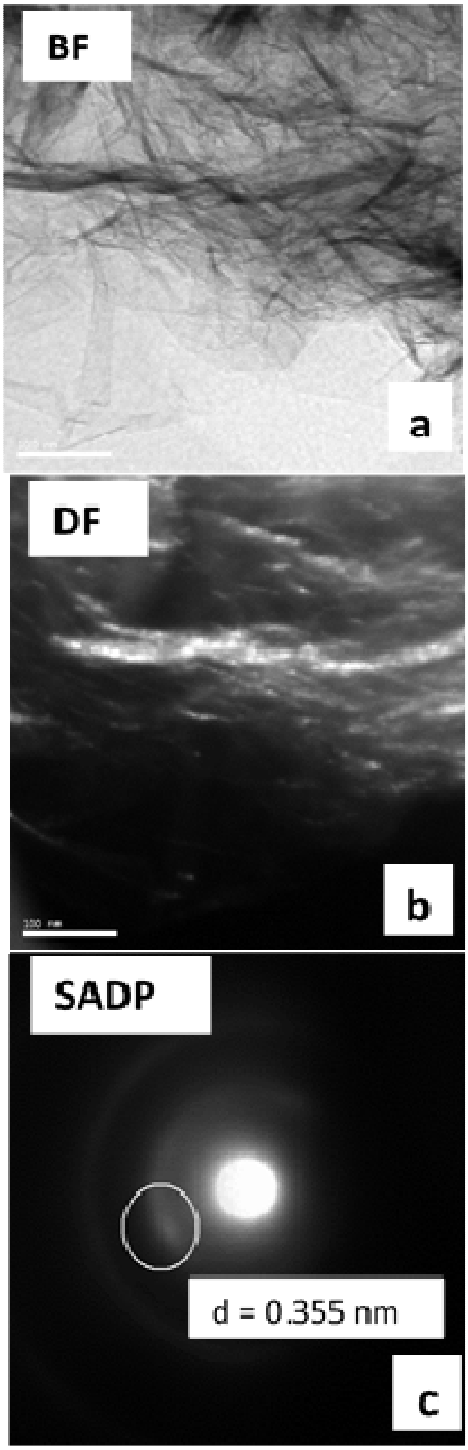

Fig. 4. TEM micrographs from FLRGO graphene platelets in BF image (a) in DF image (b) taken using diffused 002 graphene reflection shown in SADP in (c)

Rys. 4. Mikrostruktury TEM w jasnym polu (BF) (a) i w ciemnym polu (DF) (b) wykonane z rozmytego refleksu 002 grafenu FLRGO pokazanego na dyfrakcji elektronowej SADP (c)

Characterization of composites

Figure 5 shows SEM micrographs of hot pressed composites containing 1% N006 and 1% FLRGO graphene platelets. One can see that the N006 sample shows copper particles deformed during milling and the graphene additions are located at the particle boundaries. In the sample with the FLRGO fine graphene additions, the graphene particles penetrate into the copper which is not as greatly deformed.

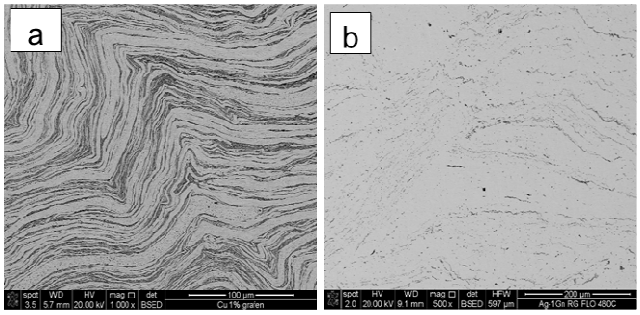

Fig. 5. SEM micrographs of vacuum hot pressed composites containing 1% N006 graphene (a) and 1% FLRGO graphene (b)

Rys. 5. Mikrostruktury SEM kompozytów prasowanych na gorąco w próżni zawierających 1% grafenu N006 (a) i 1% grafenu FLRGO (b)

These observations are confirmed by the TEM micrographs in Figure 6 where one can see large particles of N006 platelets, while the fine additions of FLRGO graphene of the size of several nanometers are distributed as smaller ones, more homogeneously within the copper grains. The diffraction pattern from graphene in Figure 6a shown as an insert shows a strongly diffused spot of basal plane of graphite, while in the sample with FLRGO graphene, one cannot see so clearly the reflections from the graphene since the inclusions are very small and the graphene reflections are absorbed by the copper. The copper shows single crystal reflections from the zone axis close to [001] and diffused in rings from deformed nanograins near the graphene platelets.

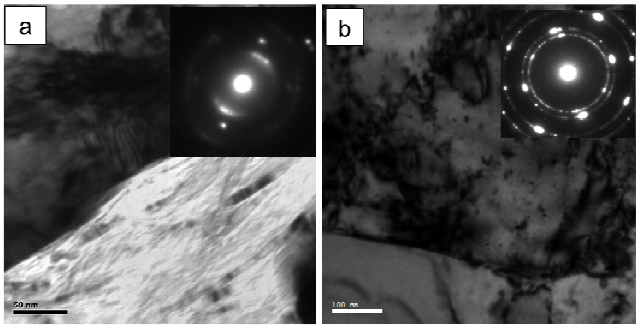

Fig. 6. TEM micrographs from hot pressed composites: a) Cu-1% N006 and b) Cu-1% FLRGO

Rys. 6. Mikrostruktury TEM kompozytów prasowanych na gorąco w próżni: a) Cu-1% N006 i b) Cu-1% FLRGO

The milling of the mixture of copper powders and MWCNT was performed up to 32 hours. Changes in the copper lattice parameter were not found up to this time

of milling but only an increase in internal stresses and refinement of the crystallites were observed in the X-ray diffraction. SEM studies of the copper powder particles after different milling times show the morphology of particle changes significantly during the first 8 hours of milling. In this period, an increase in particle size and elongation of their shape occurs. This is associated with the welding process of individual particles which is predominant in the first stage of milling. When work hardening of the particles due to collisions reaches the maximum value, the defragmentation process begins to be predominant and a decrease in particle size is observed. After the longest milling time, homogenous particles of a size of about 30 μm with an almost spherical shape were fabricated. Observation of the powder surfaces at higher magnification allowed to identify homogenously distributed MWCNTs of a size of about 1 μm of length. It indicates that MWCNTs are also subjected to deformation and fragmentation processes during milling. The longest time of milling was chosen for the sintering process of milled powders with MWCNT in order to compare their mechanical and electrical properties. Figure 7 presents a set of BF and DF TEM microstructures and corresponding SADP of the bulk composites obtained from powders milled for 5 and 32 hours (for simplification, further they will be called 5 h and 32 h composites, respectively).

Significant differences in the microstructure can be observed between these two composites. Taking into account diffraction patterns, one can see that in the case of the 5 h composite, the individual reflections can be better distinguished due to single grain orientations than in the case of the 32 h, where rings of reflections can be seen due to the fine grain structure. It indicates that the microstructure after longer milling is more refined and the grains possess texture. The DF images prove this statement. In the case of the 5 h composite, elongated grains of about 100 nm in width and 500 nm in length, while in the case of the 32 h composite almost equiaxed grains of an average size of about 131 nm can be observed. Additionally, differences are visible in the size and distribution of MWCNTs in these two composites. In the SADP images, in the case of the 5 h composite, the two diffused reflexes in shape of arcs from CNTs are present, while in the case of the 32 h composite, clear rings with individual reflexes can be seen indicating further refinement of MWCNTs. The positions in the SADP of both above diffraction reflexes have 0.34 nm interplanar spacing in real space and it very well corresponds to the (002) graphite planes. In the DF images of the 5 h composite, MWCNTs of about 200 nm length can be seen homogenously distributed between copper grains, while in the 32 h only rarely very thin tubes can be recognized. It indicates that prolonged milling leads to both strong fragmentation of the matrix as well as the carbon nanotubes. In terms of the electrical properties this phenomenon is undesirable, in contrast it can significantly improve the mechanical properties. It is therefore necessary to find a compromise between these properties. The microstructure of the 5h composite was also analyzed by HREM. Figure 8 presents the HREM image and its Fast Fourier Transform (FFT) made in the marked area and corresponding Inverse fast Fourier transform (IFFT) computed after the masking procedure. One can see the interface boundary between the copper grains with a [110] zone axis and carbon nanotubes without additional phases (oxides), however, containing some fraction of an amorphous phase. It proves the FFT image where a diffused ring can be distinguished. It can therefore be concluded that fragmentation of the carbon nanotubes is accompanied by a process of their amorphization due to an increase in the density of structural defects during the milling process.

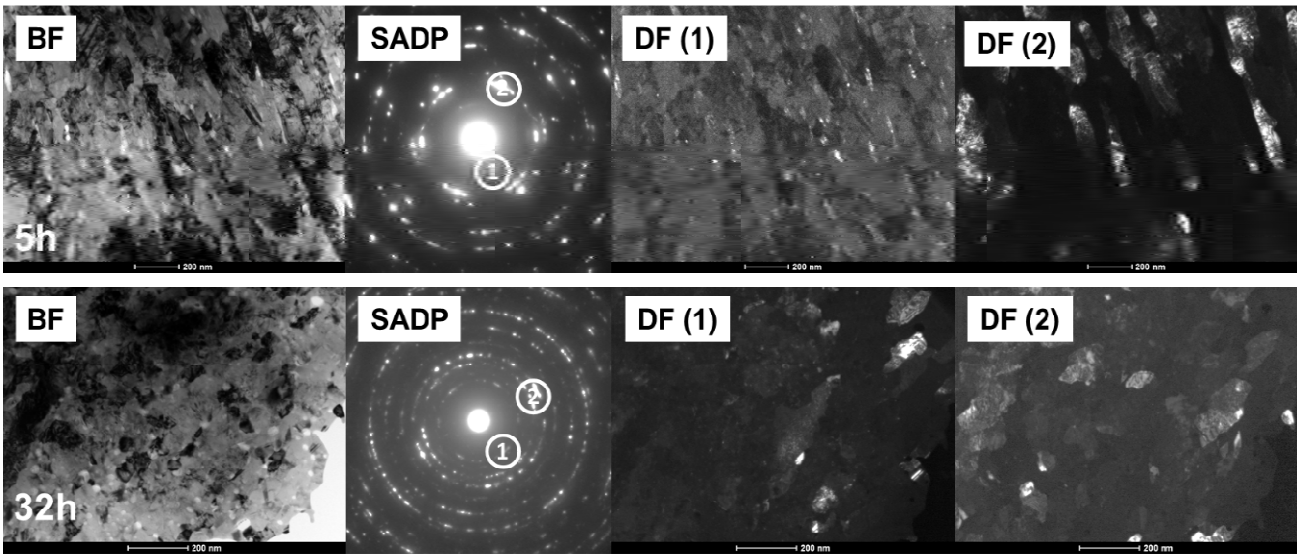

Fig. 7. Set of BF and DF TEM microstructures and corresponding SADP of bulk composites obtained from powder milled for 5 (upper row) and 32 hours (bottom row)

Rys. 7. Zestaw mikrostruktur TEM w jasnym (BF) i ciemnym (DF) polu oraz odpowiadające im dyfrakcje elektronowe z wybranych obszarów (SADP) masywnych kompozytów uzyskanych po 5 godzinach mielenia (rząd górny) i 32 godzinach mielenia (rząd dolny)

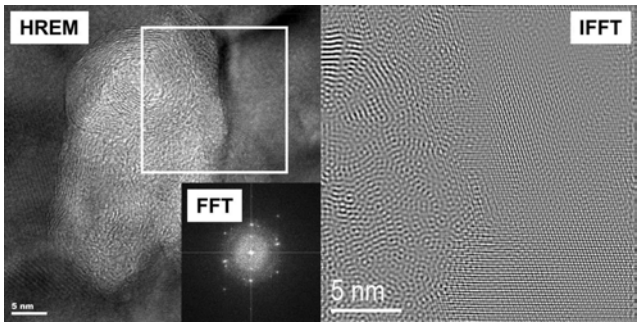

Fig. 8. HREM TEM microstructure of 5 h composite and corresponding FFT and IFFT images

Rys. 8. Mikrostruktura wysokorozdzielcza HREM TEM masywnego kompozytów uzyskanego po 5 godzinach mielenia oraz odpowiadające jej obrazy FFT i IFFT

Figure 9 shows the results of hardness measurements and electrical resistivity of composites with either nanotube or graphene platelet additions. It can be observed that the lowest electrical resistivity below 2.5 10^{-8} Ω m is obtained for composites with fine graphene platelet additions. The resistivity only slightly increases when the additions increase from 1 to 2 wt.%. The addition of CNT causes an electrical resistivity increase above 2.5 10^{-8} Ω m, and above 4 10^{-8} Ω m at a 3 wt.% CNT addition.

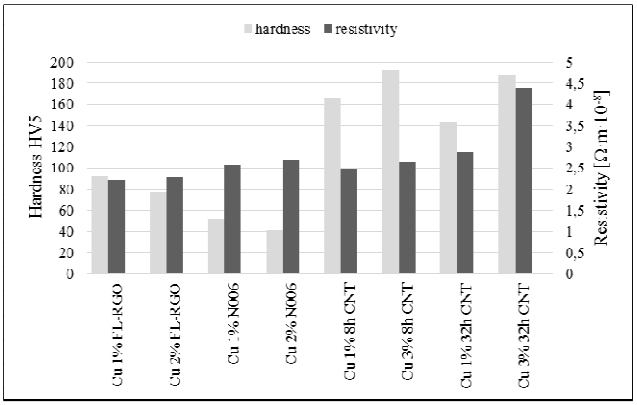

Fig. 9. Graph illustrating changes in hardness and electrical resistivity with changing amount and kind of either carbon nanotubes or graphene platelets in hot pressed copper base composites

Rys. 9. Wykres ilustrujący zmiany twardości i przewodności elektrycznej ze zmianą ilości i rodzaju płatków grafenu oraz nanorurek węglowych w kompozytach na osnowie miedzi prasowanych na gorąco

CONCLUSIONS

The addition of coarser graphene platelets in the amount of 1÷2 wt. % causes in hot pressed copper matrix composites an inhomogeneous distribution of deformed copper particles in spite of previous ball milling. Platelet conglomerates do not grow during the consolidation process. The addition of fine FLRGO platelets causes a much more homogeneous distribution within the copper particles and at the particle boundaries. It causes refinement of the copper grains near the platelets. A finer platelet addition to the copper causes less strengthening, but smaller electrical resistivity. Ball milling of the copper base powder mixture with additions of MWCNTs in the amount of 1÷3 wt.% causes their refinement up to 32 hours of milling. The carbon nanotubes are also refined. Fragmentation of the carbon nanotubes is accompanied by a process of their amorphization due an increase in the density of structural defects during the milling process. Hot pressing does not cause copper grain growth and the composites made from 32-hour milled powders show a finer grain size than those prepared from 5-hour milled powders. The additions of CNTs causes higher hardness of the composites due to the finer grain size than composites with graphene, but higher electrical resistivity most probably due to the finer grain size and amorphization of the nanotubes due to milling. The best combination of hardness and electrical conductivity was reached for the bulk composites previously milled for a maximum up to 8 hours.

Acknowledgements

Financial support from the NCBiR Research Project GRAF-TECH/NCBR/10/29/2013 is gratefully acknowledged.

REFERENCES

[1] Sie Chin Tjong, Recent progress in the development and properties of novel metal matrix nanocomposites reinforced with carbon nanotubes and graphene nanosheets, Mater. Sci. Eng. R 2013, 74, 281-350.

[2] Kim K.T., Cha S.I., Hong S.H., Hong S.H., Microstructures and tensile behavior of carbon nanotube reinforced Cu matrix nanocomposites, Mater. Sci. Eng. A 2006, 430, 27-33.

[3] Cho S., Kikuchi K., Miyazaki T., Takagi K., Kawasaki A., Tsukada T., Multiwalled carbon nanotubes as a contributing reinforcement phase for the improvement of thermal conductivity in copper matrix composites, Scr. Mater. 2010, 63, 375-378.

[4] Uddin S.M., Mahmud T., Wolf C., Glanz C., Kolaric I., Volkmer C., Höller., Wiencke U., Roth S., Fecht H.-J., Effect of size and shape of metal particles to improve hardness and electrical properties of carbon nanotube rreinforced copper and copper alloy composites, Composites Sci. Technol. 2010, 70, 16, 2253.

[5] Cho S., Kikuchi K., Kawasaki A., On the role of amorphous intergranular and interfacial layers in the thermal conductivity of a multi-walled carbon nanotube–copper matrix composite, Acta Mater. 2012, 60, 726-736.

[6] Shukla A.K., Nayan N., Murty S.V.S.N., Sharma S.C., Mondal K., Chandran P., Bakshi S.R., George K.M., Processing of copper-carbon nanotube composite powders by vacuum hot pressing technique, Mater. Sci. Eng. A 2013, 560, 365-371.

[7] Kim K.T., Cha S.I., Hong S.H., Hong S.H., Microstructure and tensile behavior of carbon nanotube reinforced Cu matrix nanocomposite, Mater. Sci. Eng. A 2006, 430, 27-33.

[8] Hassan M.T.Z., Esawi A.M.K., Metwalli S., Effect of carbon nanotube damage on the mechanical properties of aluminium

–carbon nanotube composites, Journal of Alloys and Compounds 2014, 607, 215-222.

[9] Shukla A.K., Nayan N., Murty S.V.S.N., Mondal K., Sharma S.C., George K.M., Bakshi S.R., Processing copper-carbon nanotube composite powders by high energy milling, Materials Characterization 2013, 84, 58-66.

[10] Koppad P.G., Aniruddha Ram H.R., Ramesh C.S., Kashyap K.T., Koppad R.G., On thermal and electrical properties of multiwallled carbon nanotubes/copper matrix nanonocomposites, Journal of Alloys and Compounds 2013, 12, 527-532.

[11] Yoo S.J., Han S.H., Kim W.J.. A combination of ball milling and high-ratio differential speed rolling for synthesizing carbon nanotube/copper composites, Carbon 2013, 61, 487-500.

[12] Stefov V., Nadojski M., Bogoeva-Gaceva G., Buzarovska A., Properties assessment of multiwalled carbon nanotubes: A comparive study, Synthetic Metals 2014, 197, 159-167.

[13] Madavali B., Lee J.-H., Lee J.K., Cho K.Y., Challapalli S., Hong S.-J., Effect of atmosphere and miling time on the coarsening of copper powders during mechanical milling. Powder Technol. 2014, 256, 251-256.

[14] Liu X.-Y., Xiang X.-Z., Niu F., Bai X.-J., Properties of copper/graphite/carbon nanotubes composite reinforced by carbon nanotubes, Rare Metals 2013, 32(3), 278-283.

[15] Dutkiewicz J., Ozga P., Maziarz W., Pstruś J., Kania B., Bobrowski P., Stolarska J., Microstructure and properties of bulk copper matrix composites strenghtened with various kinds of graphene nanoplatelets, Mater. Sci. Eng. A 2015, 628, 124-134.

